Ferromagnetic Exchange Coupling of Vanadium(IV) dπ Spins across Pyrimidine Rings: Dinuclear Complexes of Oxovanadium(IV) Bis(1,1,1,5,5,5-hexafluoropentane-2,4-dionate) Bridged by Pyrimidine Derivatives

Takayuki Ishida,*,† Shin-ichi Mitsubori,† Takashi Nogami,† Naoya Takeda,‡ Masayasu Ishikawa,‡ and Hiizu Iwamura§

Department of Applied Physics and Chemistry, The University of Electro-Communications, Chofu, Tokyo 182-8585, Japan, Institute for Solid State Physics, The University of Tokyo, Kashiwa, Chiba 277-8581, Japan, and The University of the Air, Wakaba, Mihama-ku, Chiba 261-8586, Japan

Received July 10, 2001

Dinuclear oxovanadium(IV) complexes bridged by pyrimidine derivatives, L[VO(hfac)$_2$]$_2$ [L = pyrimidine (PM), 4-methylpyrimidine (MPM), 4,6-dimethylpyrimidine, 4-aminopyrimidine, and quinazoline; hfac = 1,1,1,5,5,5-hexafluoropentane-2,4-dionate], were synthesized and characterized. All of them showed intramolecular ferromagnetic interaction, and the magnetic susceptibilities were analyzed on the basis of the singlet−triplet model, giving $2J/k_B = 2.2-5.5$ K. PM[VO(hfac)$_2$]$_2$ crystallized in a monoclinic space group $C2/c$ with $a = 34.092(2)$, $b = 6.9783(4)$, and $c = 16.4940(9)$ Å, $\beta = 109.104(1)°$, $V = 3707.8(4)$ Å^3, and $Z = 4$ for $C_{24}H_8F_{24}N_2O_{10}V_2$, and MPM[VO(hfac)$_2$]$_2$ gave isomorphous crystals. A semiempirical calculation study based on the determined structure suggests the presence of dπ−pπ interaction between vanadium and pyrimidine nitrogen atoms. Ferromagnetic coupling is explained in terms of a spin-polarization mechanism across the pyrimidine bridge. The intermolecular ferromagnetic interaction of PM[VO(hfac)$_2$]$_2$ can be interpreted by the contact between the spin-polarized pyrimidine moiety and the oxovanadium oxygen atom in an adjacent molecule.

Introduction

A wide variety of complexes with three-dimensional networks have been developed in which π-conjugated N-donor ligands are used for bridges (cyanide and dicyanamide anions for instance).[1−3] Control of magnetic interactions in polynuclear complexes is a key for building molecule-based magnets.[4] High-spin organic molecules (**A** and its analogues with spin sources of radicals, carbenes, or nitrenes) are accessible when nonbonding molecular orbitals are present due to π-topological symmetry of the alternant hydrocarbon skeletons.[5] Application of this strategy to transition-metal complexes is not sufficiently understood, and only a few complexes have been exploited along this approach.[6−9] Francesconi and co-workers revealed that the dinuclear titanium(III) complexes containing 2,4-dimercaptopyrimidine or its selenium analogue as a bridge exhibited ferromagnetic coupling between the titanium spins.[7] McCleverty and co-workers demonstrated that the dinuclear molybdenum(V) complexes bridged by bipyridyls showed magnetic couplings which were consistent with an anticipation from the spin polarization mechanism.[8] We planned to investigate dinuclear vanadium(IV) complexes as a prototype of ground high-spin (triplet) molecules (**B**) because all of the unpaired electron configurations of Ti^{III}, Mo^{V}, and V^{IV} are d^1 and the dπ−pπ orbital overlap seems to be essential for realization of ferromagnetic interaction based on the spin polarization effect.

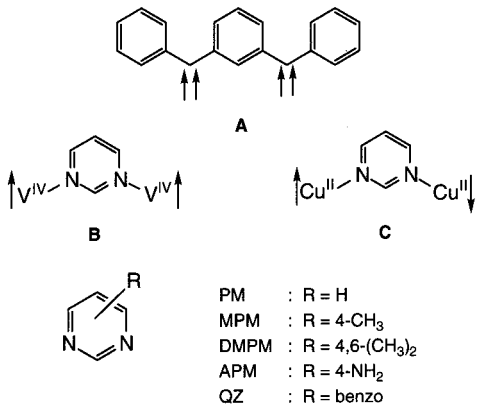

We synthesized pyrimidine-bridged dinuclear vanadium(IV) complexes L[VO(hfac)$_2$]$_2$ [L = pyrimidine (PM), 4-methyl-

* Corresponding author. Tel: +81-424-43-5490. Fax: +81-424-43-5501. E-mail: ishi@pc.uec.ac.jp.
† The University of Electro-Communications.
‡ The University of Tokyo.
§ The University of the Air.

(1) Ferlay, S.; T. Mallah, T.; Ouahés, R.; Veillet, P.; Verdaguer, M. *Nature* **1995**, *378*, 701. Sato, O.; Iyoda, T.; Fujishima, A.; Hashimoto, K. *Science* **1997**, *272*, 704.
(2) Batten, S. R.; Jensen, P.; Moubaraki, B.; Murray, K. S.; Robson, R. *Chem. Commun.* **1998**, 439. Kurmoo, M.; Kepert, C. J. *New J. Chem.* **1998**, *22*, 1515. Manson, J. L.; Kmety, C. R.; Huang, Q. Z.; Lynn, J. W.; Bendele, G. M.; Pagola, S.; Stephens, P. W.; Liable-Sands, L. M.; Rheingold, A. L.; Epstein, A. J.; Miller, J. S. *Chem. Mater.* **1998**, *10*, 2552.
(3) Kusaka, T.; Ishida, T.; Hashizume, D.; Iwasaki, F.; Nogami, T. *Chem. Lett.* **2000**, 1146.
(4) Kahn, O. *Molecular Magnetism*; VCH: New York, 1993.
(5) Iwamura, H. *Adv. Phys. Org. Chem.* **1990**, *26*, 179. Rajca, A. *Chem. Rev.* **1994**, *94*, 871. Mataga, N. *Theor. Chim. Acta* **1967**, *10*, 372. Longuet-Higgins, J. C. *J. Chem. Phys.* **1950**, *18*, 265. Crayston, J. A.; Devine, J. N.; Walton, J. C. *Tetrahedron* **2000**, *56*, 7829.
(6) Ishida, T.; Mitsubori, S.-i.; Nogami, T.; Iwamura, H. *Mol. Cryst. Liq. Cryst.* **1993**, *233*, 345. Ishida, T.; Nogami, T. *Recent Res. Devel. Pure Appl. Chem.* **1997**, *1*, 1.

10.1021/ic010730n CCC: $20.00
Published on Web 11/13/2001

pyrimidine (MPM), 4,6-dimethylpyrimidine (DMPM), 4-aminopyrimidine (APM), and quinazoline (QZ); hfac = 1,1,1,5,5,5-hexafluoropentane-2,4-dionate] and preliminarily reported their magnetic properties.[10−12] On the other hand, pyrimidine rings can also work as antiferromagnetic couplers in manganese(II),[6] iron(II),[3,13] cobalt(II),[3,6,14] nickel(II),[6,13] and copper(II)[6,15−17] complexes (**C**). A few theoretical analyses have been reported on the roles of pyrimidine as an exchange coupler.[18,19] We describe here the X-ray crystal structures of PM[VO(hfac)$_2$]$_2$ (**1**) and MPM[VO(hfac)$_2$]$_2$ (**2**) and discuss mechanisms of their intra- and intermolecular ferromagnetic exchange couplings. Spin distribution onto the pyrimidine ligands is proposed to play an important role in both intra- and intermolecular magnetic interactions.

Experimental Section

Materials. Pyrimidine ligands were purchased from TCI, Aldrich, or Wako and used without further purification. VO(hfac)$_2$ was prepared according to the literature method.[20] The following complexation of VO(hfac)$_2$ and PM is typical.

To a dichloromethane solution (15 mL) containing VO(hfac)$_2$ (0.4 mmol) was added PM (0.2 mmol) with a microsyringe. After being refluxed for 1 h, the mixture was concentrated to ca. 2 mL by a rotary evaporator and diluted with hexane (5 mL). The crude product of **1** crystallized after standing at room temperature and collected on a filter. The product was purified by repeated recrystallizations from dichloromethane−hexane.

1: yield 64%, brown plates. Anal. Calcd for $C_{24}H_8N_2O_{10}F_{24}V_2$: C, 27.66; H, 0.77; N, 2.69. Found: C, 27.36; H, 0.87; N, 2.79. **2**: yield 54%, brown plates. Anal. Calcd for $C_{25}H_{10}N_2O_{10}F_{24}V_2$: C, 28.43; H, 0.95; N, 2.65. Found: C, 28.32; H, 1.09; N, 2.80. DMPM[VO(hfac)$_2$]$_2$: yield 21%, brown powder. Anal. Calcd for $C_{26}H_{12}N_2O_{10}F_{24}V_2$: C, 29.18; H, 1.13; N, 2.62. Found: C, 28.92; H, 1.40; N, 2.61. APM[VO(hfac)$_2$]$_2$: yield 52%, brown powder. Anal. Calcd for $C_{24}H_9N_3O_{10}F_{24}V_2$: C, 27.27; H, 0.86; N, 3.98. Found: C, 27.40; H, 1.08; N, 4.05. QZ[VO(hfac)$_2$]$_2$: yield 71%, fine black plates, mp 149.5 °C. Anal. Calcd for $C_{28}H_{10}N_2O_{10}F_{24}V_2$: C, 30.79; H, 0.92; N, 2.57. Found: C, 30.68; H, 1.15; N, 2.84. The crystals were sublimed or decomposed above 140 °C during melting-point measurements except for QZ[VO(hfac)$_2$]$_2$.

X-ray Crystallographic Analysis. Diffraction data for **1** and **2** were collected on a Rigaku R-axis RAPID diffractometer with graphite-monochromated Mo Kα radiation (λ = 0.710 69 Å) at 293 K. Numerical absorption correction was applied. The initial structures were directly solved by a heavy-atom Patterson method in the teXsan program package.[21] All of the atoms including hydrogens could be found in difference Fourier maps for **1**. The atomic coordinates and thermal displacement parameters were refined anisotropically for non-hydrogen atoms and isotropically for hydrogen atoms. In the case of **2** parameters of hydrogen atoms are not included for the refinement. Full-matrix least-squares methods were applied using all of the independent diffraction data for **1** and **2**. Each trifluoromethyl group was found to possess two conformations, and these occupancies were determined by disordered models.

The crystallographic data of **1** are as follows: $C_{24}H_8F_{24}N_2O_{10}V_2$; monoclinic, *C*2/*c*; a = 34.092(2), b = 6.9783(4), c = 16.4940(9) Å; β = 109.104(1)°; V = 3707.8(4) Å^3; Z = 4; d_{calcd} = 1.867 g cm^{-3}; μ(Mo Kα) = 6.77 cm^{-1}; R_{int} = 0.032, R = 0.050 ($I > 2.0\sigma(I)$), and R_w = 0.139 (all data) for 4218 observed reflections ($R = \Sigma||F_o| - |F_c||/\Sigma|F_o|$ and $R_w = [\Sigma w(F_o^2 - F_c^2)^2/\Sigma w(F_c^2)^2]^{1/2}$). The crystal size was 0.2 × 0.08 × 0.08 mm^3. Figure 1a shows a crystallographically independent unit for **1**, in which only major conformations of the trifluoromethyl groups were drawn for the sake of clarity. The occupancies of the major conformations were 0.55, 0.78, 0.53, and 0.50 for C4, C8, C9, and C13 trifluoromethyl groups, respectively.

The crystallographic data of **2** are as follows: $C_{25}H_{10}F_{24}N_2O_{10}V_2$; monoclinic, *C*2/*c*; a = 33.866(8), b = 7.455(2), c = 16.119(4) Å; β = 109.627(4)°; V = 3833(1) Å^3; Z = 4; d_{calcd} = 1.830 g cm^{-3}; μ(Mo Kα) = 6.56 cm^{-1}; R_{int} = 0.064, R = 0.083 ($I > 2.0\sigma(I)$), and R_w = 0.192 (all data) for 4314 observed reflections. The crystal size was 0.15 × 0.15 × 0.05 mm^3. Since the cell constants of **2** were very close to those of **1**, the structure was solved by the model in which the methyl group of MPM had an occupancy of 0.5 due to the symmetry. Although the refinement for **2** was converged properly with a conformational analysis on trifluoromethyl groups similarly to the case of **1**, the *R* factors are poorer than those of **1**. The additional methyl group was found on the C2 position with an occupancy of 0.5, but four hydrogen atoms on the methyl group and on the C2 atom could not be determined. The molecular framework, symmetry, and the cell constants of **2** are sufficiently reliable for discussion.

Magnetic Measurements. Magnetic susceptibilities of polycrystalline specimens were measured on a Quantum Design MPMS SQUID magnetometer at 0.5 T in a temperature range down to 1.8 K. Magnetization curves were obtained on an Oxford Instruments Faraday balance equipped with a 7 T coil. The magnetic responses were corrected with diamagnetic blank data of the sample holder obtained separately. The diamagnetic contribution of sample itself was estimated from Pascal's constants.

The ac susceptibility was measured down to about 40 mK in a ^{3}He−^{4}He dilution refrigerator at the ac magnetic field of about 4 μT with a frequency of 127 Hz. The $M-H$ curve was recorded by an integration technique in which the difference of the voltages induced on pickup and reference coils by sweeping the magnetic field is integrated over time by a computer.[22]

Molecular Orbital Calculation. Semiempirical UHF (unrestricted Hatree−Fock) calculation on INDO (intermediate neglect of differential overlap) approximation were done on a ZINDO module in the CAChe program package.[23] The atomic coordinates were available from the X-ray crystallographic analysis. A hypothetical molecule, PM·VO(hfac)$_2$, has 40 atoms, 147 atomic orbitals, and 191 electrons in the valence shell. The surface of the molecular orbitals was drawn at the 0.05 e Å^{-3} level. In calculation on the twist angle dependence of the

(7) Francesconi, L. C.; Corbin, D. R.; Clauss, A. W.; Hendrickson, D. N.; Stucky, G. D. *Inorg. Chem.* **1981**, *20*, 2078.
(8) Ung, V. A.; Couchman, S. M.; Jeffery, J. C.; McCleverty, J. A.; Ward, M. D.; Totti, F.; Gatteschi, D. *Inorg. Chem.* **1999**, *38*, 365.
(9) Oshio, H.; Ichida, H. *J. Phys. Chem.* **1995**, *99*, 3294. Oshio, H. *J. Chem. Soc., Chem. Commun.* **1991**, 240.
(10) Mitsubori, S.-i.; Ishida, T.; Nogami, T.; Iwamura, H. *Chem. Lett.* **1994**, 285.
(11) Mitsubori, S.-i.; Ishida, T.; Nogami, T.; Iwamura, H.; Takeda, N.; Ishikawa, M. *Chem. Lett.* **1994**, 685.
(12) Ishida, T.; Mitsubori, S.-i.; Nogami, T.; Ishikawa, Y.; Yasui, M.; Iwasaki, F.; Iwamura, H.; Takeda, N.; Ishikawa, M. *Synth. Met.* **1995**, *71*, 1791.
(13) Zusai, Z.; Kusaka, T.; Ishida, T.; Feyerherm, R.; Steiner, M.; Nogami, T. *Mol. Cryst. Liq. Cryst.* **2000**, *343*, 127.
(14) Nakayama, K.; Ishida, T.; Takayama, R.; Hashizume, D.; Yasui, M.; Iwasaki, F.; Nogami, T. *Chem. Lett.* **1998**, 497.
(15) Yasui, M.; Ishikawa, Y.; Akiyama, N.; Ishida, T.; Nogami, T.; Iwasaki, F. *Acta Crystallogr. B* **2001**, *57*, 288. Feyerherm, R.; Abens, S.; Günther, D.; T. Ishida, T.; Meissner, M.; Meschke, M.; Nogami, T.; Steiner, M. *J. Phys.: Condens. Matter* **2000**, *12*, 8495.
(16) Ezuhara, T.; Endo, K.; Matsuda, K.; Aoyama, Y. *New J. Chem.* **2000**, *24*, 609.
(17) Omata, J.; Ishida, T.; Hashizume, D.; Iwasaki, F.; Nogami, T. *Inorg. Chem.* **2001**, *40*, 3954.
(18) Mohri, F.; Yoshizawa, K.; Yamabe, T.; Ishida, T.; Nogami, T. *Mol. Eng.* **1999**, *8*, 357.
(19) Takano, Y.; Onishi, T.; Kitagawa, Y.; Soda, T.; Yoshioka, Y.; Yamaguchi, K. *Int. J. Quantum Chem.* **2000**, *80*, 681.
(20) Su, C.-C.; Reed, J. W.; Gould, E. S. *Inorg. Chem.* **1973**, *12*, 337. Selbin, J.; Maus, G.; Johnson, D. L. *J. Inorg. Nucl. Chem.* **1967**, *29*, 1735.
(21) *teXsan*: *crystal structure analysis package*; Molecular Structure Corp.: The Woodlands, TX, 1985, 1999.
(22) Nakazawa, Y.; Tamura, M.; Shirakawa, N.; Shiomi, D.; Takahashi, M.; Kinoshita, M.; Ishikawa, M. *Phys. Rev. B* **1992**, *46*, 8906.
(23) *ZINDO*, CAChe 3.9; Oxford Molecular Group; Oxford, U.K., 1996. Zerner, M. C.; Loew, G. H.; Kirchner, R. F.; Mueller-Westerhoff, U. T. *J. Am. Chem. Soc.* **1980**, *102*, 589 and references therein.

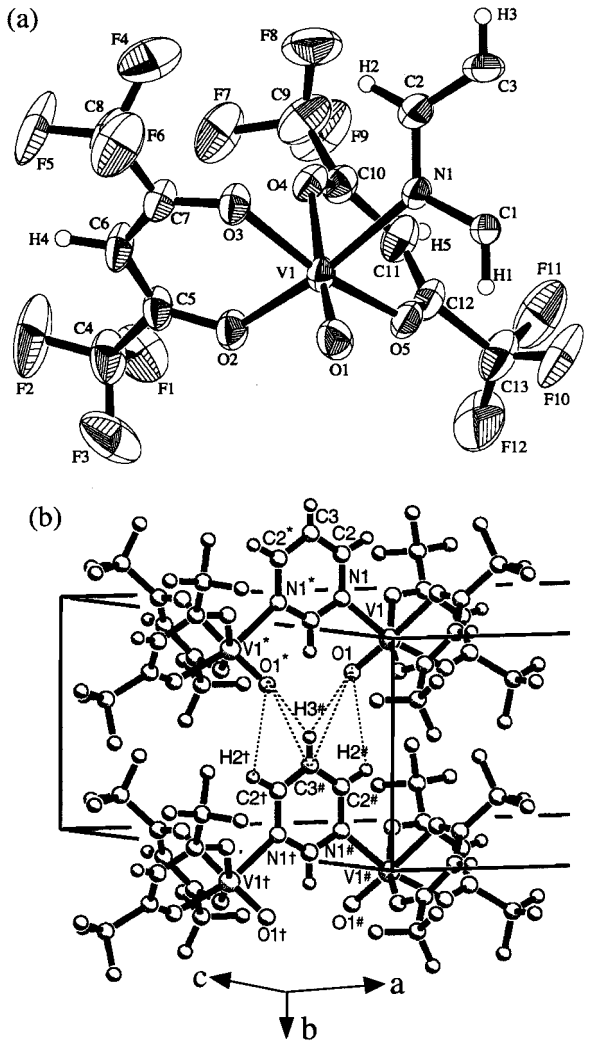

Figure 1. (a) ORTEP drawing of PM[VO(hfac)$_2$]$_2$ (**1**) with thermal ellipsoids at the 30% probability level. Only major conformations of the trifluoromethyl groups are drawn for the sake of clarity. Atomic numberings are also shown. (b) Nearest neighboring molecular arrangement of **1**. Relatively short interatomic distances are shown with dotted lines. The distances are 3.04(4), 3.03(4), and 3.582(5) Å for O1···H2$^{\#}$, O1···H3$^{\#}$, and O1···C3$^{\#}$, respectively. Symmetry operation codes: for *, $-x, -y, -z + 1/2$; #, $x, y + 1, z$; †, $-x, y + 1, -z + 1/2$.

spin density distribution around the V1−N1 bond, the rigid structures of the PM and VO(hfac)$_2$ moieties were used.

Results

Structures of 1 and 2. We obtained single crystals of **1** and **2** which are suitable for X-ray structure analysis. The analysis reveals that the two molecular structures are essentially identical with the same symmetry, except for the additional methyl group in **2**. The difference of molecular arrangements will be discussed later in connection with the presence or absence of intermolecular magnetic interaction. The crystallographically independent unit and atomic numbering of **1** are shown in Figure 1a. A half of **1** is crystallographically independent with a 2-fold axis through C1−C3. Selected interatomic distances and angles are listed in Table 1. The vanadium ion has an octahedral coordination sphere, and the oxovanadium oxygen and PM nitrogen atoms are located in a cis configuration. The crystal consists of a racemic mixture of $\Delta-\Delta$ and $\Lambda-\Lambda$ enantiomers, which are related by inversion symmetry in a *C*2/*c* space group.

It is crucial for the analysis of magnetic interaction which site, axial or equatorial, each PM nitrogen is coordinated to.

Table 1. Selected Bond Lengths (Å) and Angles (deg) for PM[VO(hfac)$_2$]$_2$ (**1**)

V1−N1	2.163(2)	C1−N1	1.326(3)
V1−O1	1.583(3)	N1−C2	1.325(4)
V1−O2	2.010(2)	C2−C3	1.369(4)
V1−O3	1.985(2)	O2−C5	1.253(4)
V1−O4	2.159(2)	O3−C7	1.255(4)
V1−O5	1.999(2)	O4−C10	1.244(4)
		O5−C12	1.248(4)
N1−V1−O1	93.5(1)	O1−V1−O2	101.2(1)
N1−V1−O2	165.1(1)	O1−V1−O3	100.6(1)
N1−V1−O3	90.82(9)	O1−V1−O4	176.2(1)
N1−V1−O4	83.02(9)	O1−V1−O5	96.0(1)
N1−V1−O5	86.29(9)		
O1−V1−N1− C1	42.3(2)	O3−V1−N1−C1	142.9(2)
$\phi_{1,4}$[a]	42.6(2)	$\phi_{3,4}$[a]	98.3(2)
$\phi_{2,4}$[a]	47.4(2)		

[a] Dihedral angles between two least-squares planes. The suffixes 1−4 denote the planes defined by the following atoms: 1, V1, O1, O2, O4, and N1; 2, V1, O5, O2, O3, and N1 (equatorial plane); 3, V1, O1, O3, O4, and O5; 4, C1, N1, C2, and C3 (pyrimidine plane).

Although the V−N distance is 2.163(2) Å which is largest among the coordination distances, we cannot distinguish which is axial or equatorial only from the distances, because the covalent and ion radii of each atom are different. The direction of the oxovanadium oxygen (O1) and O4 is usually assigned to be axial from the ligand field theory under octahedral symmetry. Actually, the coordination bond of V1−O4 (2.159(2) Å) is significantly longer than those of V1−O2, −O3, and −O5 (1.99−2.01 Å). The PM nitrogen is assigned to be at an equatorial position, and the magnetic orbital is d_{xy}.

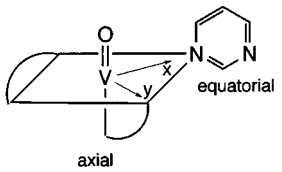

Two related mononuclear compounds, (pyridine)VO(acac)$_2$[24] and (γ-picoline)VO(acac)$_2$,[25] were reported previously, where acac denotes pentane-2,4-dionate. In contrast to the case of **1** and **2**, the nitrogen atoms are coordinated at the axial position, i.e., the trans position to the oxovanadium oxygen. The V−N bond lengths are 2.45−2.48 Å in the acac complexes, which is fairly longer than that of **1**, because of the distortion of an elongated octahedron. However, the geometrical arguments of the acac compounds also concluded the magnetic orbital to be d_{xy}.

The PM plane in **1** is located almost perpendicular to the O1−O3−O4−O5 plane as indicated by the dihedral angles of 98.3(2)° (Table 1). The dihedral angles between the PM bridge and two coordination planes, O1−O2−O4−N1 and O5−O2−O3−N1, are also important for the interpretation of magnetic interaction. As Table 1 shows, the PM plane is largely canted from the V1−O1−O2−O4−N1 and V1−O5−O2−O3−N1 planes with an angle of 42.6(2)°.

Compounds **1** and **2** are isomorphous, and the cell constants are very close to each other. The additional methyl group does not affect the coordination structure. Since the PM moiety has a staggered conformation around V1−N1 bond in the original

(24) Shao, M.; Wang, L.; Tang, Y. *Kexue Tongbao* **1984**, *29*, 759.
(25) Shao, M.; Wang, L.; Tang, Y. *Huaxue Xuebao (Acta Chim. Shinica)* **1983**, *41*, 985.

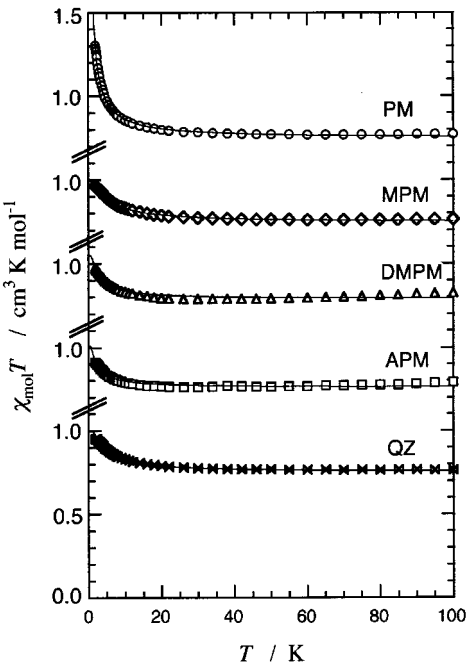

Figure 2. Temperature dependence of the product $\chi_{mol}T$ for L[VO(hfac)$_2$]$_2$ containing various pyrimidines. For abbreviation of the ligands, see the text. The solid lines represent the fits to the equation based on the singlet−triplet model.

form of **1**, the methyl group in **2** can be accommodated into an open space without any cost of geometrical deformation. Therefore, it is reasonably understood that the crystal of **2** has an only slightly larger (3.4%) cell volume.

However, the *b* axis of **2** is significantly longer (6.8% or $\Delta b = 0.48$ Å) than that of **1**. Several intermolecular contacts within 3 Å are found between fluorine atoms in these crystals. The hfac groups can hardly act as a magnetic coupler. Caneschi and co-workers reported that various metal bis(hfac) salts bridged with imidazoline-1-oxyl 3-oxide radicals formed one-dimensional magnetic structure,[26] in which interchain metal−metal exchange interaction is prohibited by intervening trifluoromethyl groups. In this study we have to focus on short interatomic distances with respect to VO−PM−VO cores. As Figure 1b shows, the nearest neighboring molecules are related by the *b*-axis translation. Relatively short distances are found between oxovanadium oxygen atom (O1) and pyrimidine hydrogen (H2, H3) and carbon atoms (C3), as indicated by dotted lines in Figure 1b. No other meaningful contacts were found. In the case of **2**, the methyl group on C2 separates these contacts, as evidenced by the anisotropic elongation in the *b* direction.

The molecular structures of L[VO(hfac)$_2$]$_2$ (L = DMPM, APM, and QZ) could not be determined because of their poor crystalline nature. Their V^{IV}−PM−V^{IV} skeleton and the coordination spheres may be similar to those of **1** and **2** viewing from the magnetic properties as shown below.

Magnetic Properties of Pyrimidine-Bridged Complexes. Figure 2 shows the temperature dependence of the product of temperature and molar magnetic susceptibility per a dinuclear molecule ($\chi_{mol}T$) for the five pyrimidine-bridged complexes obtained here. In a high-temperature region, the $\chi_{mol}T$ values are close to 0.75 cm^3 K mol^{-1} for all complexes. Although precise *g* values are calculated from theoretical fitting, these $\chi_{mol}T$ values indicate that the *g* values of the vanadium(IV) ions are very close to 2.0, suggesting that orbital contribution is negligible. We apply the Bleaney−Bowers formula[27] to the present system, similarly to the analysis of the magnetic properties of isomeric pyrazine (PZ) bridged complex, PZ[VO(hfac)$_2$]$_2$, which was proposed to possess an identical coordination sphere.[28]

Table 2. Best-Fit Parameters for the Magnetic Measurements of L[VO(hfac)$_2$]$_2$[a]

L	g	$2Jk_B^{-1}$/K	Θ/K	ref
PM	1.99	4.46	0.49	this work
MPM	1.99	5.48		this work
DMPM	2.05	2.88		this work
APM	2.01	2.22		this work
QZ	2.00	4.50		this work
PZ[b]	1.92	−55.0		ref[e]
MPZ[c]	1.99	−19.4		ref[e]
DMPZ[d]	1.93	−11.6		ref[e]

[a] For the fitting equations and abbreviations, see the text. [b] Pyrazine. [c] Methylpyrazine. [d] 2,5-Dimethylpyrazine. [e] Haddad, M. S.; Hendrickson, D. N.; Cannady, J. P.; Drago, R. S.; Bieksza, D. S. *J. Am. Chem. Soc.* **1978**, *101*, 898.

pyrazine

The $\chi_{mol}T$ values increased with decreasing temperature for all of the complexes investigated here, indicating that the $S = 1/2$ spins of vanadium(IV) ions are ferromagnetically coupled. The experimental $\chi_{mol}T$ values approached from the isolated $S = 1/2$ spin-only value (0.75 cm^3 K mol^{-1}) to the $S = 1$ spin-only value (1.00 cm^3 K mol^{-1}) with $g = 2$. Assuming that the temperature dependence of the $\chi_{mol}T$ is ascribable only to the spin−spin coupling, we analyze these data by the following formula:[27]

$$\chi_{mol} = \frac{2Ng^2\mu_B{}^2}{k_BT}\frac{1}{3 + \exp(-2J/k_BT)} \qquad (1)$$

where the singlet−triplet energy gap corresponds to 2*J*. The best fit *J* parameters are summarized in Table 2, and the calculated curves are superposed in Figure 2. Positive *J* values imply the presence of ferromagnetic interaction within a molecule; i.e., the molecule is a ground high-spin (triplet) species. The $2J/k_B$ values are 2.2−5.5 K.

In the case of **1**, the $\chi_{mol}T$ value exceeded the theoretical triplet value at 1.8 K. The data were analyzed on eq 2 by introducing a Weiss mean field parameter Θ to eq 1. We obtained $\Theta = +0.49$ K together with $g = 1.99$ and $2J/k_B = 4.46$ K for **1**.

$$\chi_{mol} = \frac{2Ng^2\mu_B{}^2}{k_B(T - \Theta)}\frac{1}{3 + \exp(-2J/k_BT)} \qquad (2)$$

To clarify whether the spins are coupled in an intramolecular fashion, we measured the magnetization curves. Figure 3a shows that the magnetization of **2** at 3.0 K fell exactly on the Brillouin function with $S = 1$, clearly demonstrating that the molecule has a ground triplet state without any appreciable intermolecular magnetic interaction.

(26) Caneschi, A.; Gatteschi, D.; Lalioti, N.; Sangregorio, C.; Sessoli, R. *J. Chem. Soc., Dalton Trans.* **2000**, 3907. Caneschi, A.; Gatteschi, D.; Lalioti, N.; Sangregorio, C.; Sessoli, R.; Venturi, G.; Vindigni, A.; Rettori, A.; Pini, M. G.; Novak, M. A. *Angew. Chem. Int. Ed. Engl.* **2001**, *40*, 1760.

(27) Bleaney, B.; Bowers, K. D. *Proc. R. Soc. London, Ser. A* **1952**, *214*, 451.

(28) Haddad, M. S.; Hendrickson, D. N.; Cannady, J. P.; Drago, R. S.; Bieksza, D. S. *J. Am. Chem. Soc.* **1978**, *101*, 898.

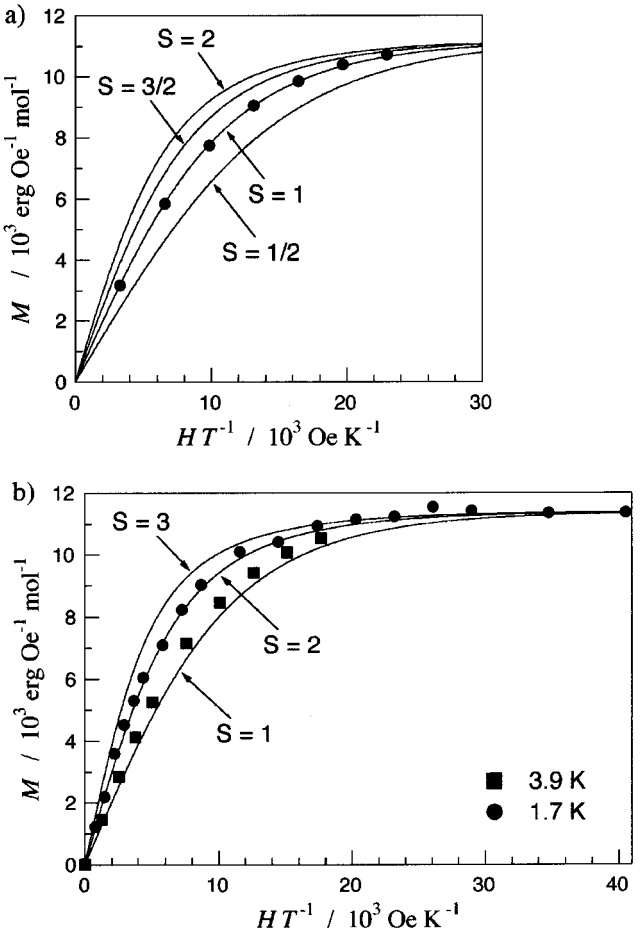

Figure 3. (a) Magnetization curves of MPM[VO(hfac)$_2$]$_2$ at 3.0 ± 0.1 K. The solid lines represent theoretical curves with $S = 1/2$, 1, 3/2, and 2 ($g = 2.0$). (b) Magnetization curves of PM[VO(hfac)$_2$]$_2$ at 1.7 ± 0.1 K (circles) and at 3.9 ± 0.1 K (squares). The solid lines represent theoretical curves with $S = 1$, 2, and 3 ($g = 2.0$).

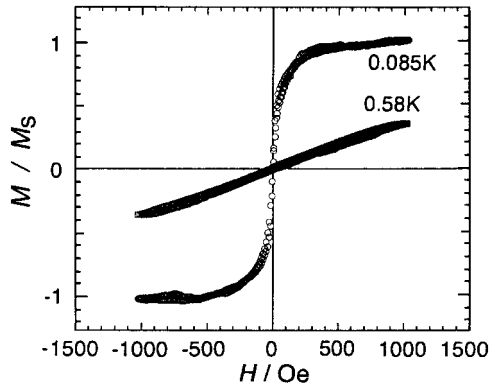

Figure 4. Magnetization curves of PM[VO(hfac)$_2$]$_2$ at 0.085 and 0.58 K.

On the other hand, the magnetization curves of **1** exceeded that of the Brillouin function with $S = 1$ and the saturation was more remarkable at lower temperature (Figure 3b). This finding is consistent with the positive Θ obtained above (Table 2). These facts indicate the presence of intermolecular ferromagnetic interaction as well as intramolecular one. In fact, as the magnetic measurements below 1.8 K revealed, the ac magnetic susceptibility starts to diverge at around 0.14 K.[11] The $M-H$ curve at 0.085 K shows an S-shaped curve (Figure 4) whereas a paramagnetic feature was observed at 0.58 K. The S-shaped curve strongly suggests that ferromagnetic ordering takes place. The coercive field at 0.085 K was very small (<5 Oe). From the crystal structure analysis, we can only find a uniform one-dimensional chain structure consisting of the dinuclear complexes along the *b* axis (Figure 1b). The intermolecular magnetic interaction along the *b* axis is safely assumed to be ferromagnetic. However, interchain interaction is hardly explained by the crystal structure. Since the vanadium(IV) spins have practically no magnetic anisotropy as indicated by the *g* values close to 2.0, the bulk magnetism may depend on the low-dimensional structure leading to a possible dipolar interaction among the chains.

We have to make some argument regarding other contributions (e.g. zero-field splitting) to the temperature dependence of $\chi_{mol}T$. We proved the exact $S = 1$ Curie behavior of **2** as shown by the Brillouin curve in Figure 3a and the plateau of the $\chi_{mol}T$ value around 2 K in Figure 2. Figure 2 also shows stepwise behavior from the exact $S = 1/2$ spin-only value to the exact $S = 1$ spin-only value for **2** with a decrease of temperature. These findings indicate that the main contribution of this temperature dependence should be attributed to spin−spin coupling interaction. However, a small contribution of zero-field splitting which may be operative below 1.8 K cannot be eliminated.

To compare the function of isomeric pyrazine (PZ) as a magnetic exchange coupler, we also measured magnetic properties of PZ[VO(hfac)$_2$]$_2$ and found the intramolecular antiferromagnetic coupling with $2J/k_B = -67$ K.[10] This finding is in good agreement with those reported by Hendrickson and coworkers;[28] L[VO(hfac)$_2$]$_2$ (L = pyrazine, methylpyrazine, 2,5-dimethylpyrazine) showed antiferromagnetic coupling between vanadium(IV) spins across the pyrazine ring (Table 2), and the pyrazine nitrogen atom was suggested to be located at an equatorial position from the X-ray powder diffraction study. Therefore, we can conclude that pyrimidine and pyrazine bridges can work as ferromagnetic and antiferromagnetic couplers, respectively, in which the bridging bases are located at equatorial positions of VO(hfac)$_2$ in common.

Discussion

The present conclusion is entirely compatible to the organic compounds, xylylenes; *m*- and *p*-xylylenes are ground high-spin and low-spin molecules, respectively.[5] For further discussion on the detailed exchange mechanism in the bis-VO(hfac)$_2$ system, we performed a semiempirical molecular orbital calculation on these complexes on the basis of the geometry determined by the X-ray crystal structure analysis. We calculated on a hypothetical mononuclear species, PM·VO(hfac)$_2$. The UHF treatment in INDO[23] calculation of PM·VO(hfac)$_2$ gave the singly occupied molecular orbital (SOMO) with the orbital energy of −8.007 eV (Figure 5). The SOMO resides on the O5−O2−O3−N1 equatorial plane, which justifies the geometrical definition from the structural analysis. Apparently the SOMO is mainly contributed from a t_{2g} dπ (d_{xy}) orbital of the vanadium ion, whose symmetry is preferable for the V−PM conjugation.

The coefficients of the atomic orbitals in the PM moiety are so small that their lobes could not appear in Figure 5. Instead, calculated spin density may give valuable information about what happens in the vanadium−PM conjugation. The spin densities at V1, N1, C1, N1*, C2*, C3, and C2 are calculated to be +1.150, −0.182, +0.197, −0.178, +0.190, −0.214, and +0.194, respectively (symmetry operation code for *: $-x$, y, $-z + 1/2$). The UHF treatment tends to overestimate polarized

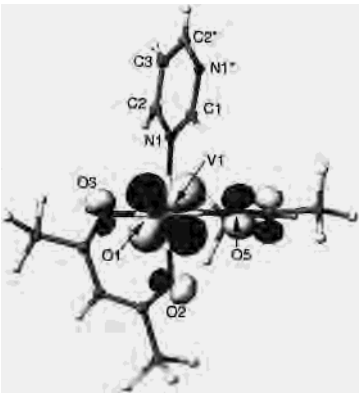

Figure 5. Surface of the singly occupied molecular orbital of PM·VO(hfac)$_2$ based on UHF calculation in the INDO method. The atomic coordinates determined by the X-ray crystallographic study were used.

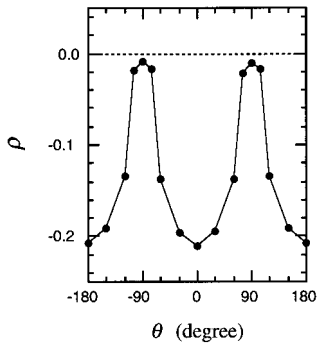

Figure 6. Spin density (ρ) on N1* as a function of dihedral angle (θ) of O1−V1−N1−C1 calculated with UHF/INDO. The solid line is drawn for a guide to the eye.

spin densities.[29] The sign of the spin densities in the present study is confirmed to alternate throughout the PM π-electron network. The ferromagnetic coupling in the present complexes can be understood as follows. Once a negative spin density is induced at the coordinated nitrogen atom (N1), alternating spin densities are induced on the π-electron network of a six-membered PM ring. In the real dinuclear compounds, N1* which carries polarized negative spin density is coordinated to an adjacent vanadium ion, and consequently, the vanadium ion is positively spin polarized. On the other hand, when a pyrazine ring is used as a bridge, a neighboring vanadium ion is negatively spin polarized, i.e., antiferromagnetically correlated.

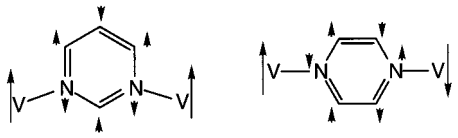

To check the role of the dπ−pπ conjugation between V and PM, we calculated the variation of the spin density distribution as a function of the twist angle around the V−N bond. Calculated spin densities will give reliable comparison within calculation study despite the overestimation. The twist angle θ is defined by the dihedral angle of O1−V1−N1−C1. The experimental angle in **1** is 42.3(2)°. As Figure 6 shows, the calculated spin density on N1* oscillates twice in a cycle. The molecule has no symmetrical element around V1−N1 (2-fold axis or mirror plane) and therefore the calculated density must not be the same between −180 and 0° and 0 and 180°. However the profiles of the two area are quite similar to each other, indicating the presence of a local π-type overlap through the V1−N1 bond on the MO level. A parallel arrangement between the vanadium d_{xy} and nitrogen p_z orbitals ($\theta = 0$ and $\pm$ 180°) is ideal for the maximum orbital overlap, while practically no spin density is polarized when $\theta = \pm 90°$. In the present system, medium overlap is expected from the staggered conformation (θ = ca. 45°) and, therefore, the π-electron system of PM moderately participates in the SOMO.

As described above, the crystals of **1** and **2** have an isostructure but the intermolecular magnetic interactions are different. Assuming that the pyrimidine ring has an appreciable polarized spin density, the different interactions are reasonably explained as follows. The UHF/INDO calculation indicates the presence of positive and negative spin densities at H3 and O1, respectively. The crystal structure analysis reveals the interatomic distances of 3.03(3) and 3.582(5) Å for H3$^{\#}$···O1 and C3$^{\#}$···O1, respectively (symmetry operation code for #: $x, y + 1, z$). Nonzero atomic orbital overlap between O1 and H3$^{\#}$ can be expected because the O1···H3 distances are only slightly larger than the sum of the van der Waals radii. Such a contact gives rise to a weak hydrogen bond, i.e., local antiferromagnetic coupling between small spin densities on O1 and H3$^{\#}$ atoms. Thus, a spin polarization scheme can be drawn as V1(↑)-N1-(↓)-C2(↑)-C3(↓)-H3(↑)···O(↓)═V(↑). Two vanadium spins are ferromagnetically correlated. In the crystal of **2**, the methyl group on C2 prohibit the H3$^{\#}$···O1 interaction due to the steric hindrance. Compound **2** behaves as an ideal paramagnet with $S = 1$.

As mentioned in Introduction, there are several instances of pyrimidine-bridged complexes showing antiferromagnetic interactions. The copper(II) nitrate complexes containing PM bridges are extensively investigated.[15,18] The equatorial−equatorial coordination was found in the antiferromagnetic PM-bridged complex, $[PM{\cdot}Cu(NO_3)_2{\cdot}(H_2O)_2]_n$.[15] The σ-type orbital overlaps between copper $d_{x^2-y^2}$ and nitrogen n orbitals on both sides give rise to an antiferromagnetic superexchange through the PM orbital(s).[18] A similar σ pathway is proposed also in copper(II)−pyrazine complexes.[30] In sharp contrast to the copper case, complexes **1** and **2** possessing a symmetrical equatorial−equatorial coordination structure show ferromagnetic interaction through a π pathway. Yamaguchi and co-workers suggested that the exchange interaction should be divided into two terms: the spin polarization effect and superexchange mechanism (spin delocalization effect).[19] The π- and σ-pathways are theoretically explained in connection with the spin polarization and superexchange mechanism, respectively; the spin polarization effect controls the magnetic coupling of the V^{IV} complexes with only dπ spins, whereas the superexchange is dominantly operative in the Cu^{II} complexes having dσ spins.

Acknowledgment. This work was supported by a Grant-in-Aid for Scientific Research on Priority Areas of "Molecular Conductors and Magnets" (No. 730/11224204) and by a Grant-in-Aid for Scientific Research (No. 13640575) from the Ministry of Education, Culture, Sports, Science, and Technology of Japan.

Supporting Information Available: Crystallographic data (excluding structure factors) for the structures of **1** and **2**, in CIF format. This material is available free of charge via the Internet at http://pubs.acs.org.

IC010730N

(29) Zheludev, A.; Barone, V.; Bonnet, M.; Delley, B.; Grand, A.; Ressouche, E.; Rey, P.; Subra, R.; Schweizer, J. *J. Am. Chem. Soc.* **1994**, *116*, 2019.

(30) Kuramoto, H.; Inoue, M.; Emori, S.; Sugiyama, S. *Inorg. Chem. Acta* **1979**, *32*, 209.